J Mater Sci (2011) 46:7931–7935
DOI 10.1007/s10853-011-5927-4

LETTER

A voltage-dependent investigation on detachment process for free-standing crystalline TiO_2 nanotube membranes

Guohua Liu · Nils Hoivik · Kaiying Wang · Henrik Jakobsen

Published online: 14 September 2011

Introduction

TiO_2 nanotube (TNT) arrays have attracted considerable scientific interests because of their photoelectric properties and technological importance for diverse applications as solar cells [1–4], photocatalysis [5–7], gas sensors [8], hydrogen generation from water splitting [6], and composite nano-membranes [9, 10]. Among various synthesis methods, electrochemical anodization is an excellent approach to fabricate TNT arrays due to its simplicity, low cost, and tunable morphology [11]. However, the nature of as-prepared TNT membrane adhered on opaque Ti foil restricts their feasibility for the applications such as tube filling [9, 10], biofiltration, flow-through photocatalytic reactions [5], and front illumination in solar cells [2–4]. After detachment from the substrate, free-standing TNT membranes show high performance due to the absence of a blocking layer [2, 4]. The TNT membrane can be directly used or attached on foreign substrates for the above applications.

So far, different techniques have been proposed for preparing free-standing TNT membranes from Ti substrates, including ultrasonic splitting [8], solvent evaporation [12, 13], chemically assisted delamination [6, 14–16], selective metal dissolution [5, 17], and voltage transition at the end of anodization [18–22]. Generally speaking, these processes fabricated amorphous and fragile TNT membranes. The amorphous characteristic of these membranes hampered their applications and the crystallized TNT membrane is desirable for practical devices. To get the crystallized TNT membranes, attempts such as selective dissolution of the amorphous layer between the desired crystalline TNT arrays and Ti substrate [3], adjusting electrolyte temperature in multi-step anodic processes [23] have also been explored. The success of the former is due to the different resolvability of materials, while the different mechanical stability and etching contrast between the layers account for the latter's detachment. Nevertheless, the fabrication of large-area and free-standing crystalline TNT membranes is still a challenge.

In this article, a handy experimental procedure was reported to fabricate free-standing crystalline TNT membranes. The concept is outlined in Fig. 1 (1–4). The ordered TNT arrays are firstly fabricated under optimized parameters, after an annealing and followed by a second (detachment) anodization step, free-standing crystalline TNT membranes are detached from the substrate without any cracks. This method is a reliable technique for fabricating free-standing TNT membranes without the needs for any complicated processes or dangerous chemicals. At the same time, different from previous studies, we have systematically investigated the effects of voltage on the detachment process of free-standing crystalline TNT membranes.

Experimental section

Ti foils were cut into required size ($\sim$15 mm $\times$ 35 mm $\times$ 0.3 mm, 99.8% purity, obtained from Baoji Titanium Industry Co., Ltd, China), degreased and cleaned by sonication in acetone, isopropanol, and deionized water for 10 min during each step. After drying, the backside of Ti foil was covered by a Scotch tape, rinsed by water, and exposed to UV radiation about 10 min for cleaning. Then,

G. Liu · N. Hoivik · K. Wang (✉) · H. Jakobsen
Department of Micro and Nano Systems Technology, Vestfold University College, Horten 3184, Norway
e-mail: Kaiying.Wang@hive.no

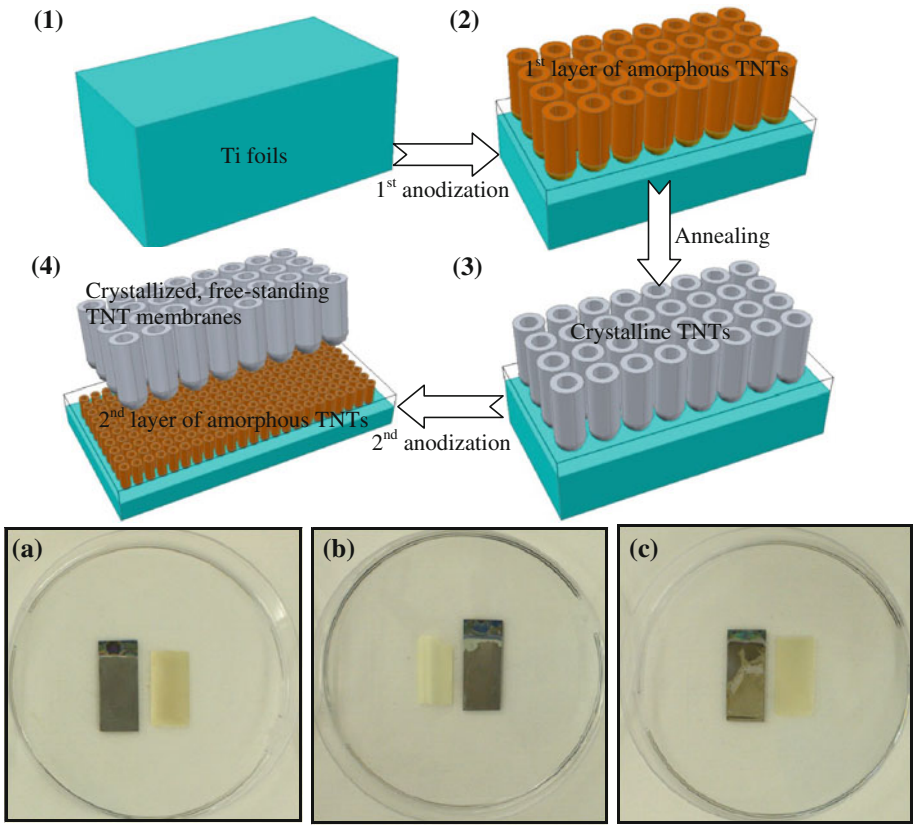

Fig. 1 Schematic illustration of the fabrication process for free-standing crystalline TNT membranes (*1–4*) and **a–c** the three resulting samples are firstly anodized at 60 V/24 h, then annealing at 500 °C/3 h, followed by another anodization at 20 V/60 min, 60 V/30 min, and 100 V/10 min, respectively

it was put into a polyflon cell with an area of 4 cm^2 exposed to the electrolyte. Ethylene glycol with 0.5 wt% ammonium fluoride (NH_4F) and 3 vol% water was used as electrolyte. The first anodization was started with growth of ordered TNT arrays on Ti foil under 60 V for 24 h, followed by sonic cleaned in ethanol to remove the electrolytes and annealed at 500 °C for 3 h to crystallize the TNT arrays. Then, the annealed samples were anodized again in the same stock electrolyte with another voltage (e.g., 20, 60, 100 V). After detecting the detachment occurs over time to each case, the samples were picked out and rinsed by ethanol to remove the electrolytes, finally dried in air. The morphology of the TNT membranes was characterized by a Philip EX-30 scanning electron microscope (SEM). X-ray diffraction analysis (Bruker AXS D8 Discover with a normal θ–2θ scan, Cu-Kα radiation) was performed for phase identification.

Results and discussion

Figure 1a–c shows the photographs of free-standing crystalline TNT membranes and their substrates with various detachment voltages (second anodization). The membrane geometry was defined by the first anodization (60 V/24 h) [20], but the applied voltages in second anodization step were 20, 60, and 100 V, respectively, corresponding to the sample a, b, and c. It can be seen that the membranes formed with white color, free of cracks and only slightly bending upon air drying. This bending effect may be ascribed to the absence of barrier layer at tube bottom, where compressive stress is exerted.

Figure 2 shows the top view, cross section, and bottom view SEM images of the above three membranes. From the top view and cross section images in Fig. 2a–c, it can be observed that all membranes (the insets of Fig. 2a–c) display a thickness of 18 μm and the average inner diameter of 140 nm, which are not influenced by the second anodization step. This phenomenon indicates that crystallized layer shows high resistance to chemical etching from the electrolyte. Figure 2d–f shows the surface of Ti substrates after detachment and bottom morphology of the membranes. It can be seen in Fig. 2d and its inset that the membrane detached at low voltage (under 20 V for 60 min) preserves their tube morphology and the bottom of tubes are closed, and a non-ordered compact oxide layer is present on the bottom of membrane. As shown in Fig. 2e, the nanotube bottom ends are opened partly in 30 min with the detachment voltage equals to 60 V. On the other hand, all bottom ends of the nanotube are homogenously opened at the high detachment voltage (100 V), and the through-hole diameter is about 50 nm as present in the inset of

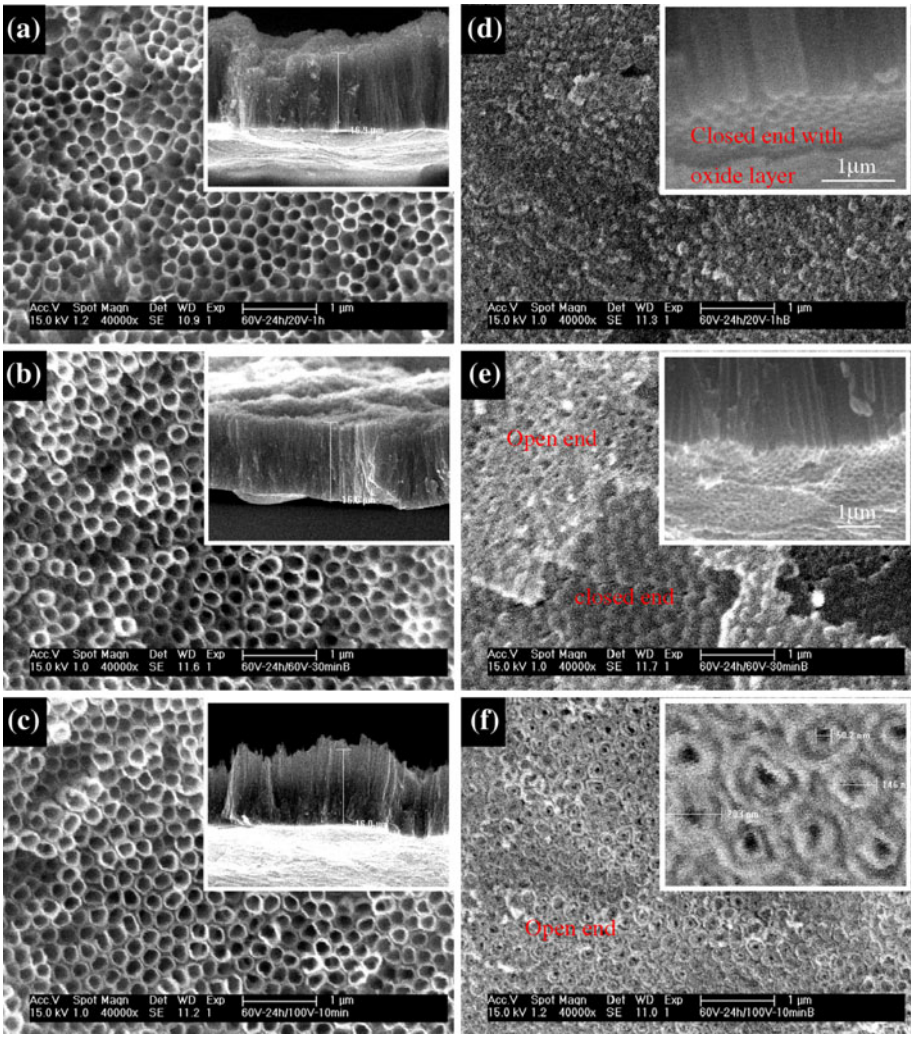

Fig. 2 **a–c** Top view, cross section (*inset*), and **d–f** bottom view images for the membrane (Fig. 1a–c)

Fig. 2f. Besides, the detachment process at high voltage is faster than that of the low voltage, and it only needs about 10 min.

To clarify the detachment mechanism of the free-standing TNT membranes, top-view SEM images of the membranes (Fig. 3a–c) and the images of underlying TNT layer remaining on substrate (Fig. 3d–f) were further analyzed. We can see that the tip wall thickness of the TNT on membrane is about 15 nm. However, the wall thickness and inner diameters of the underlying tube on substrate are 10, 25, 45 nm and 30, 60, 80 nm corresponding to the 20, 60, and 100 detachment voltage, respectively. The interface structures of membranes before detachment might be presumed as the schematic diagrams in Fig. 3. The possible detachment mechanism of the TNT arrays from the substrate can be explained as follows: a TNT layer prepared under a set of parameters leads to a specific geometry, the underneath layer may be initiated at the bottom of a tube [24], or in the spaces between the tubes [25]. The crystallized/amorphous oxide interface forms from various anions (F^-, O^{2-}, OH^-) and metal cations Ti^{n+} combined in different ways. The relatively fast migration of fluoride ions as compared with other ions (such as O^{2-}) induced a poor adhesion between the layers [26]. Furthermore, different from previous studies, the local acidification and gas evolution produced by transition voltage [17] and mechanical contrast account for the detachment of present study. Therefore, all methods can effectively detach the TNT membrane. But the membrane detachment more likely occurs below the interface (as marked by dashed line) at low voltage and above the interface at high voltage due to sharp contrast of material properties and the resulting structure. To the middle voltage (60 V), the detachment is randomly distributed over the interface.

X-ray diffraction (XRD) patterns were further used to characterize the crystal structure of the membranes. Standard patterns of Ti (JCPDS file 44-1294) and anatase TiO_2 (JCPDS file 84-1286) were plotted in Fig. 4 for

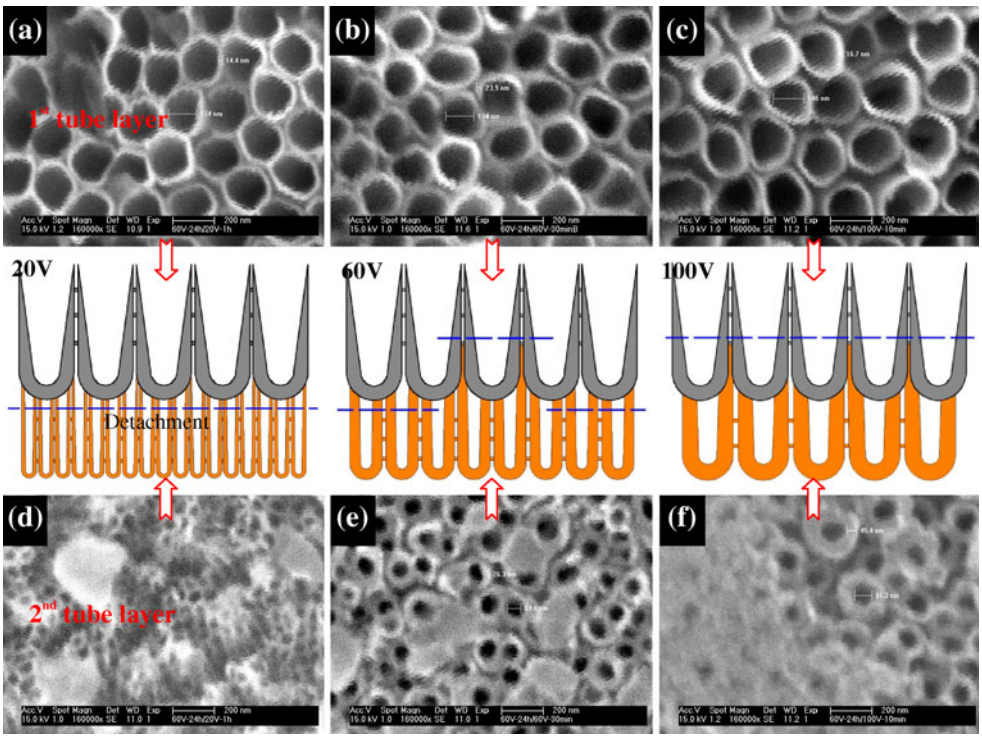

Fig. 3 The presumed structure before detachment, **a–c** top view images of the membrane and **d–f** the left layer on corresponding substrates

comparison. It shows that the preferential crystallographic orientation of the metallic Ti substrates is (103), the grain size of the underlying titanium substrate evaluated by Scherrer equation [27] is about 194.8 nm. The as-prepared TNT film is amorphous and only diffraction peaks of Ti can be found in Fig. 4a. In general, as the annealing temperature increases from room temperature to 800 °C, the phase of titanium oxide changes as amorphous → anatase → rutile. To form anatase TiO_2, annealing at 330–500 °C for 1–3 h in an oxygen ambient is a common procedure in literatures [28, 29]. After calcination at 500 °C for 3 h, more X-ray diffraction patterns are clearly observed in Fig. 4b, which can be referred to anatase phase. In contrast, for the crystallized free-standing TNT membrane, the diffraction peaks of Ti substrate disappear and all of the peaks can be attributed to the anatase TiO_2 phase (Fig. 4c), the strong diffraction peaks at $2\theta = 25.5°$, 38.1°, 48.3° can be identified, respectively, to the (101), (004), (200) crystal faces. The grain size of the anatase TiO_2 is about 81.6 nm, which was supposed no relevance to the grain size of the Ti foil but depended on the annealing temperature [28].

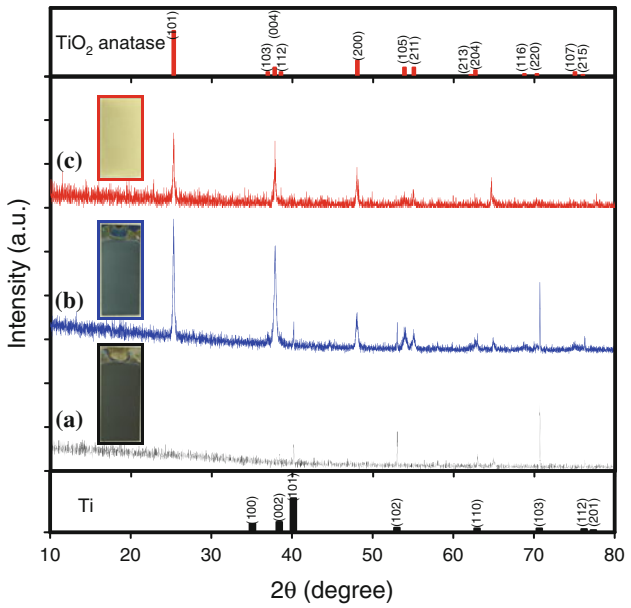

Fig. 4 XRD patterns of (**a**) as-prepared and (**b**) annealed TNT arrays on Ti substrates and **c** free-standing crystalline TNT membranes

Conclusions

A voltage-dependent investigation has been performed for the detachment process of free-standing crystalline TNT membrane. In this process, crystallized TNT membranes with high ordered nanotubes were effectively detached from Ti substrate by taking advantage of different mechanical stability between the layers. The membrane detached at low voltage preserves its nanotube morphology and the bottom of tubes are closed, while through-hole membrane with fast detachment can be obtained at a high detachment voltage. All the resulting membranes feature

high-quality surfaces and this method opens new prospects for application in photoelectric devices, high performance hydrogen sensors, photocatalysis, and drug release systems.

Acknowledgments The authors are grateful to Zekija Ramic and Ragnar D. Johansen for help of the experimental set up, Tormod Vinsand and Knut Aasmundtveit for help with SEM, Vishnukanthan Venkatachalapathy in MiNalab of Oslo University for help with XRD chractarization. The author GHL also acknowledge financial support from KD program at the Vestfold University College, Oslofjord Fund and NorFab in Norway.

References

1. Li LL, Chen YJ, Wu HP, Wang NS, Diau EW (2011) Energy Environ. Sci. doi:10.1039/c0ee00474j
2. Banerjee S, Misra M, Mohapatra SK, Howard C, Mohapatra SK, Kamilla SK (2010) Nanotechnology 21:145201
3. Chen QW, Xu DS (2009) J Phys Chem C 113:6310
4. Mor GK, Shankar K, Paulose M, Varghese OK, Grimes CA (2006) Nano Lett 6:215
5. Albu SP, Ghicov A, Macak JM, Hahn R, Schmuki P (2007) Nano Lett 7:1286
6. Mor GK, Shankar K, Paulose M, Varghese OK, Grimes CA (2005) Nano Lett 5:190
7. Varghese OK, Paulose M, LaTempa TJ, Grimes CA (2009) Nano Lett 9:731
8. Paulose M, Varghese OK, Mor GK, Grimes CA, Ong KG (2006) Nanotechnology 17:398
9. Fang D, Huang KL, Liu SQ, Luo ZP, Qing XX, Zhang QG (2010) J Alloys Compd 498:37
10. Mohapatra SK, Banerjee S, Misra M (2008) Nanotechnology 19:315601
11. Shin Y, Lee S (2009) Nanotechnology 20:105301
12. Wang J, Lin ZQ (2008) Chem Mater 20:1257
13. Ali G, Yoo SH, Kum JM, Kim YN, Cho SO (2011) Nanotechnology 22:245602
14. Lin CJ, Yu YH, Liou YH (2009) Appl Catal B 93:119
15. Park JH, Lee TW, Kang MG (2008) Chem Commun 2008:2867. doi:10.1039/B800660A
16. Wang DA, Yu B, Wang CW, Zhou F, Liu WM (2009) Adv Mater 21:1964
17. Albu SP, Ghicov A, Berger S, Jha H, Schmuki P (2010) Electrochem Commun 12:1352
18. Wang DA, Liu LF (2010) Chem Mater 22:6656
19. Kant K, Losic D (2009) Phys Status Solidi RRL 3:139
20. Li SQ, Zhang GM (2010) J Ceram Soc Jpn 118:291
21. Jo Y, Jung I, Lee I, Choi J, Tak Y (2010) Electrochem Commun. 12:616
22. Yuan XL, Zheng MJ, Ma L, Shen WZ (2010) Nanotechnology 21:405302
23. Lin J, Chen JF, Chen XF (2010) Electrochem Commun 12:1062
24. Macak JM, Albu S, Kim DH, Paramasivam I, Aldabergerova S, Schmuki P (2007) Electrochem Solid-State Lett 10:K28
25. Yasuda K, Schmuki P (2007) Electrochem Commun 9:615
26. Singh S, Festin M, Barden WRT, Xi L, Francis JT, Kruse P (2008) ACS Nano 2:2363
27. Langford JI, Wilson AJC (1978) J Appl Cryst 11:102
28. Sreekantan S, Hazan R, Lockman Z (2009) Thin Solid Films 518:16
29. Cheng Q, Ahmad W, Liu GH, Wang KY (2011) In: Proc. of 11th IEEE international conference on nanotechnology, Portland Marriott, August 15–18, 2011, Portland, OR, p 1589